Applied Catalysis B: Environmental 224 (2018) 973–982

Contents lists available at ScienceDirect

Applied Catalysis B: Environmental

journal homepage: www.elsevier.com/locate/apcatb

Review

Nonradical reactions in environmental remediation processes: Uncertainty and challenges

Xiaoguang Duan[a], Hongqi Sun[b,*], Zongping Shao[a,c], Shaobin Wang[a,*]

[a] Department of Chemical Engineering, Curtin University, GPO Box U1987, WA, 6845, Australia
[b] School of Engineering, Edith Cowan University, 270 Joondalup Drive, Joondalup, Perth, WA, 6027, Australia
[c] State Key Laboratory of Materials-Oriented Chemical Engineering, Nanjing Tech University, No.5 Xin Mofan Road, Nanjing, 210009, PR China

ARTICLE INFO

Keywords:
Nonradical reaction
Advanced oxidation processes
Water treatment
Environmental remediation

ABSTRACT

Recent discoveries of nonradical oxidation in aqueous-phase advanced oxidation processes (AOPs) have induced tremendous interest in environmental remediation of wastewater, whereas different findings from a variety of investigations have also raised severe controversies in the occurrence and mechanism of the nonradical reaction. Hence, critical understandings of the nonradical reaction will significantly advance the knowledge and its application for catalytic oxidation and wastewater treatment. In this review, we would like to present state-of-the-art research on nonradical pathways in persulfate-based AOPs, with emphases on the controversial methodologies for identifying the oxygen reactive species (ROS), ambiguous reaction mechanisms, intrinsic impacts of metal/carbon catalysts and organic substrates in the nonradical-based catalytic oxidation reactions. Moreover, further research directions on mechanistic investigation of the nonradical pathway with rational experimental design and advanced strategies, as well as the potential applications of the nonradical system are proposed.

1. Introduction

Worldwide environmental crises coming along with the rapid industrialization and civilization urge green and advanced technologies for a healthy living environment and sustainable future. Effective control and elimination of harmful contaminants in polluted aquatic systems (rivers, lakes, and oceans) and recycling use of domestic and industrial wastewaters have become the leading strategies. To this end, versatile state-of-the-art technologies have been developed in recent years for remediation of various organic pollutants such as dyes, phenolics, antibiotics, and pesticides in water matrices. For instance, physical approaches such as adsorption and flocculation can easily enrich the harmful substances in water from one phase to another for a further treatment [1–3]. Biodegradation treatment is another cost-effective technology for aerobic/anaerobic metabolism of organic substances in sanitary sewage from household and factory production [4–6]. Additionally, advanced oxidative processes (AOPs) are more powerful techniques aiming at complete decomposition of organic contaminants in an aqueous system into carbon dioxide and water, or as a preliminary treatment process for transforming the highly resistant and toxic compounds into less harmful and mineralized products for the subsequent bioprocessing [7,8].

AOPs generally utilize the highly reactive species generated from photocatalysis, electrochemistry, or superoxides for oxidative destruction of organic molecules [9–11]. For chemical oxidation based–AOPs, it is usually believed that free radicals, such as hydroxyl (·OH), sulfate ($SO_4^{\cdot -}$), and superoxide ion radicals ($O_2^{\cdot -}$), generated from various activated superoxides (ozone, persulfates, and hydrogen peroxide, etc.) are the primary reactive oxygen species (ROSs) leading to the organic degradation. This is because ROSs possess higher redox potentials than their parent superoxides. For example, Fenton reaction and ozonation have been widely applied in industrial applications using hydroxyl radicals generated from hydrogen peroxide (H_2O_2) and ozone (O_3) activations. The hydroxyl radicals are capable of almost non-selectively decomposing a variety of organic substances in aqueous systems. Besides, sulfate radical-based AOPs (SR-AOPs) are a Fenton-like oxidative system for wastewater remediation. The sulfate radicals can be produced from peroxymonosulfate (PMS) and peroxydisulfate (PDS) and manifest a greater redox potential (2.5–3.1 V) and longer life time (30–40 ms) than hydroxyl radicals (1.8–2.7 V, $<$ 1 μs) and are more applicable to a wider pH range than Fenton reactions (pH = ~ 3) [12,13]. However, it is still mysterious if other oxidative pathways, apart from the free radical oxidation, also occur and contribute concurrently to the organic degradation in AOPs.

A nonradical oxidative pathway was first discovered in the Gif chemistry. It was found that homogeneous Fe^{2+}/H_2O_2 produced not

* Corresponding authors.
E-mail addresses: h.sun@ecu.edu.au (H. Sun), shaobin.wang@curtin.edu.au, wang@exchange.curtin.edu.au (S. Wang).

https://doi.org/10.1016/j.apcatb.2017.11.051
Received 26 August 2017; Received in revised form 8 November 2017; Accepted 18 November 2017
Available online 21 November 2017
0926-3373/

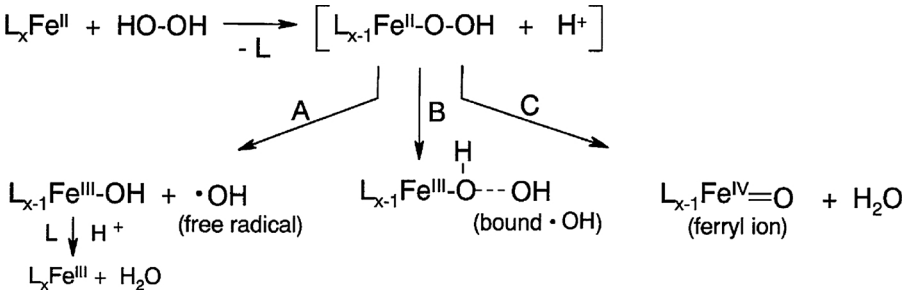

Fig. 1. The oxidative species in Fe^{2+}/H_2O_2 systems.

only the highly reactive hydroxyl radicals (Eq. (1)), but also other oxidative species in the oxidation reactions as shown in Fig. 1 [14]. In the presence of ferrous chelates, the Fenton system was discovered to be immune to the hydroxyl radical scavenger (tert-butanol), whereas the confined hydroxyl radicals (with the ferrous complex) and high-valence ferry ions (Fe^{V+}, Eq. (2)) were identified as the intrinsic oxidative species by spin-trapping electron paramagnetic resonance (EPR) and quenching experiments [15–17]. The ferry ion with a mild redox potential was utilized as a selective oxidant for activation of C—H bond in versatile hydrocarbon conversions in the Gif chemistry [14,18]. Such Fenton-like chemistry was dominated by the reactivity of iron species rather than hydroxyl radicals [19]. More importantly, the radical and nonradical reaction pathways of the Fenton system could be switched or manipulated by absolute proton concentration (Eq. (3)) and variation of pH, which subsequently determined the reactivity and selectivity of the oxidative system [20,21].

$$Fe^{2+} + H_2O_2 \rightarrow Fe^{3+} + {}^{\circ}O\,H + HO^{-} \quad (1)$$

$$Fe^{2+} + H_2O_2 \rightarrow (Fe^{IV} = O)^{2+} + H_2O \quad (2)$$

$$(Fe^{IV} = O)^{2+} + H^{+} \rightarrow (Fe^{IV} - OH)^{3+} \rightarrow Fe^{3+} + HO^{-} \quad (3)$$

Nevertheless, the nonradical oxidation with Fenton reagents were applied in organic synthesis in the past few decades. However, little attention has been paid to its occurrence in the popular radical based AOPs in environmental remediation. Since the reports of the nonradical oxidative pathways upon N-doping in carbocatalysis-driven PMS activation [22] and CuO/PDS system [23], researchers have demonstrated great enthusiasm in exploring the novel nonradical reactions and re-evaluating the hydroxyl and sulfate radical-based systems in previous studies. The nonradical oxidation has been revealed to be an oxidation reaction occurring on the catalyst surface region, which is different from the radical-based oxidation taking place in the bulk solution. The nonradical reactive species were usually considered to be resistant to the popular radical scavengers (methanol, ethanol, and tert-butanol, etc.) and selective to the electron-rich organic compounds, therein demonstrating a particular sensitivity to the organic substrates with a mild redox potential. Currently, nonradical processes have been reported in versatile oxidative systems, especially in PMS and PDS activations on both nanocarbons and metal oxides, nevertheless, in controversial mechanisms.

In this critical review, we will discuss the progress of the nonradical reactions in AOPs, with an emphasis on the persulfate-based systems. The controversial methodologies of experimental design for identification of the oxygen reactive species (radical/nonradical/singlet oxygen) will be illustrated and compared. The ambiguous reaction pathways and the active sites of metal/carbon catalysts will be identified and discussed. Therefore, this review aims at providing citical comments on the future research for new advances and applications of nonradical reactions in AOPs.

2. Overview of recent progresses in nonradical oxidation

2.1. Nonradical oxidation in PMS activation

PMS activation for oxidative degradation of contaminants can be achieved in homogeneous and heterogeneous systems using different materials. The nonradical processes were recently discovered in the PMS-based AOPs, which were believed as a sulfate radical–dominated system. Jiang's group found that *p*-benzoquinone (p-BQ) could activate PMS for sulfamethoxazole oxidation in alkaline conditions [24]. In the quenching tests, the introduced radical scavengers could barely influence the oxidative efficiency of sulfamethoxazole (SMX), indicating that the p-BQ/PMS/base system was not relying on hydroxyl and sulfate radicals but singlet oxygen ($^1O_2$). Chemical trapping with diphenylanthracene (DTA) on HPLC and spin trapping with 2,2,6,6,-tetramethyl-4-piperidinol (TMP) on electron paramagnetic resonance (EPR) also witnessed the existence of singlet oxygen. The addition of sodium azide (NaN_3), a quenching agent of singlet oxygen, dramatically inhibited the oxidation, further confirming the primary role of the singlet oxygen for SMX degradation. Moreover, the mechanism of PMS activation on carbonyl group of benzoquinone was proposed in Eqs. (4)–(8). A dioxirane intermediate was involved (Eq. (7), the rate-limiting step) and further reacted with PMS to produce the singlet oxygen (Eq. (8)) [24–26]. Bedsides, it was discovered that p-BQ exhibited the highest activity among the ketones, and the catalytic activity of the carbonyl group may lie in the texture of carbon substrates (ring numbers and functionalities), which determines the electrophilicity of adjacent oxygen atoms for nucleophilic attack by PMS molecules [24,27].

$$OH^{-} + HSO_5^{-} \rightleftharpoons SO_5^{2-} + H_2O \quad (4)$$

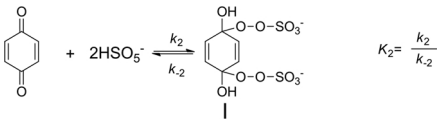

(5)

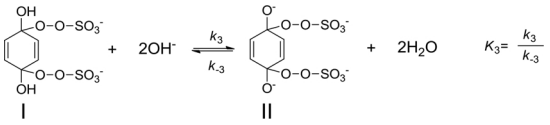

(6)

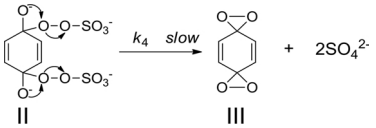

(7)

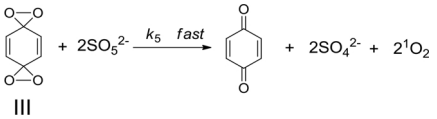

(8)

Qi et al. further reported that a base itself could activate PMS to generate superoxide radical ($O_2^{\cdot -}$) and singlet oxygen via Eqs. (9)–(16) for oxidation of acid orange 7 (AO7) [28]. These reactive species were *in situ* captured by different spin trapping agents on EPR. Interestingly, in a lower concentration range of NaOH at 0.6–1.0 mM, sodium azide only partially slowed down the decolorization rate of

AO7, whereas p-BQ, the quenching agent of superoxide radical, completely terminated the oxidation. The results suggested that both the superoxide radicals and singlet oxygen contributed to the AO7 oxidation. However, the reaction rate was decreased at a higher dosage of NaOH (6.0 mM). Meanwhile, methanol, tert-butanol, and sodium azide did not present any inhibitory effect, while benzoquinone was still effective as a quenching agent. Therefore, it could be suggested that the oxidative system was dominated by superoxide radicals at higher pH conditions, according to the fact that the coupling of two superoxide radicals to produce singlet oxygen (Eq. (16)) could be inhibited. Besides, hydrogen peroxide decomposition rate in Eq. (12) was so low that the coupling of superoxide radical and hydroxyl radical to generate singlet oxygen might be insignificant. Later, Lou et al. reported that the base activation of PMS could be impressively promoted by adding polyphosphates, even though the intrinsic role of the polyphosphates is still ambiguous [29]. It is worthwhile pointing out that the addition of p-BQ in Qi's study [28] completely terminated the oxidation process in NaOH/PMS system. This is different from Jiang's report [24], where p-BQ would synergistically activate PMS to generate singlet oxygen in basic conditions for enhanced oxidative capacity. Thus, it can be deduced that the role of p-BQ in PMS activation may be sensitive to its dosage and pH conditions.

$$HSO_5^- \rightarrow H^+ + SO_5^{2-},\ pKa = 9.4 \quad (9)$$

$$HSO_5^- + H_2O \rightarrow H_2O_2 + HSO_4^- \quad (10)$$

$$2SO_5^{2-} + 2H^+ \rightarrow H_2O_2 + 2SO_4^{2-} \quad (11)$$

$$H_2O_2 \rightarrow H^+ + HO_2^-,\ pKa = 11.65 \quad (12)$$

$$H_2O_2 \rightarrow 2^{\circ}OH \quad (13)$$

$$^{\circ}O\,H + H_2O_2 \rightarrow HO^{\circ}_2 + H_2O \quad (14)$$

$$HO^{\circ}_2 \rightarrow H^+ + O^{\circ-}_2 \quad (15)$$

$$O^{\circ-}_2 + {}^{\circ}O\,H \rightarrow {}^1O_2 + OH^- \quad (16)$$

$$2O^{\circ-}_2 + 2H^+ \rightarrow H_2O_2 + {}^1O_2 \quad (17)$$

Sun et al. first employed pristine reduced graphene oxide (rGO) as a metal-free PMS activator for degradation of organic contaminants in an aqueous system [30]. The electron-rich ketonic groups located on the grain boundaries of graphene were proposed to be the active sites, which are able to mediate a redox cycle to simultaneously produce sulfate/hydroxyl radicals (electron acceptor) and peroxymonosulfate radical ($SO_5^{\cdot -}$) (electron donor) [30,31]. Duan et al. further investigated other nanocarbons (such as single/multi-walled carbon nanotubes (SW/MW-CNT), cubic mesoporous carbon (CMK-3), annealed nanodiamond (AND), and defective graphene) and found that all these carbonaceous materials can be utilized as effective PMS activators [32,33]. However, it was also proved that the nanocarbons with diverse carbon configurations and surface chemistry exhibited quite different sensitivities toward radical quenching treatment as shown in Fig. 2 [32]. More specifically, introducing excess methanol would completely terminate the oxidation process for MWCNTs and CMK-3, whereas a high reaction rate of organic oxidation was still achieved for AND and defective graphene. This phenomenon implies that a significant contribution to the degradation from a new reaction pathway occured, which was not completely dependent on reactive radicals. It was suggested that the defective edges were the active sites to mediate PMS activation via a nonradical pathway [32]. Different from the intact graphene network with free-flowing π electrons, the carbon atoms at the edging sites remained sp^2-conjugation with unpaired electrons in a 'localized state', which were able to strongly interact with the small molecules to form an attached complex [32,34,35]. Theoretical calculations also suggested that PMS molecules presented a great adsorption tendency on zigzag and armchair edges of graphene with stretched peroxide O—O bond without dissociation into sulfate radicals (on C═O), forming a reactive intermediate that might account for the organic oxidation [32].

Moreover, Sun et al. found that nitrogen-doping could remarkably enhance the catalytic performance of graphene in PMS activation [36,37]. To exclude the implications of the defects and oxygen groups in graphene-derived materials, a highly graphitic SWCNT with ultralow oxygen level was employed as the carbon precursor. It was unveiled that a minor N-doping level (0.80 at.%) could result in a 57-fold enhancement in organic oxidation rate [22]. More surprisingly, the radical quenching tests evidenced that the N-doping of carbon nanotubes impressively altered the oxidative system from radical-based (SWCNT/PMS) degradation to a nonradical pathway dominated system (N-SWCNT/PMS) as shown in Fig. 3a and b. This is because nitrogen atoms possess a higher electronegativity than carbon atoms ($\chi_N = 3.04$ *vs* $\chi_C = 2.55$), and the doped nitrogen would then attract electrons from the adjacent carbon giving rise to the positively charged carbon domains [38,39]. These activated carbon atoms would strongly interact with the PMS to form a highly reactive complex for organic oxidation via direct electron abstraction without producing sulfate/hydroxyl radicals (Fig. 3c). Liang et al. further detected the occurrence of singlet oxygen as well as the trace amount of sulfate and hydroxyl radicals on N-doped graphene [40,41]. The carbonyl groups at the edging sites of N-doped graphene were supposed to be the active centers to mediate PMS to generate singlet oxygen (similar to p-BQ), whereas the N-doping promoted PMS to form an oxidative intermediate as illustrated in Fig. 4 [42]. Thus, multi-reaction pathways (radicals, singlet oxygen, activated PMS) could be involved in carbon/PMS catalysis systems.

A similar mechanism was also reported by Wang et al. on ferric carbide encapsulated N-doped carbon nanotubes [43]. It should be noted that in these carbon-induced and nonradical dominated oxidative systems with singlet oxygen and/or activated superoxide complex, trace level of sulfate and hydroxyl radicals were still detectable by EPR and partially contributed to organic oxidation. However, it is difficult to quantitatively estimate the different roles of singlet oxygen and the surface activated PMS (reactive complex) which may co-exist in the nonradical pathways for organic oxidation.

Lee and co-workers reported that Al_2O_3 and TiO_2 supported noble metal nanoparticles (Pd, Pt, Ag, and Au) were able to activate PMS via a nonradical mechanism, where the metal nanocrystals served as an electron conductor to promote the charge transport from the organic (electron donor) to the co-adsorbed PMS molecules (electron acceptor) via the catalyst surface [44]. In this scenario, PMS could be hardly decomposed by the catalysts without the co-existence of the organic compound. The activity of the noble metals follows an order of Ag < < Au ≈ Pt < Pd, and TiO_2 supported Pd or Pt was found to exhibit a better reactivity and stability than those supported on Al_2O_3 [44]. Different from the nonselective sulfate radical-based system of Co^{2+}/PMS, the oxidation capacity of the nonradical process in Pd/PMS impressively depended on the substrates of the organics. For example, Pd-Al_2O_3/PMS was highly oxidative to phenol and chlorophenols but moderately efficient to bisphenol A (BPA) and carbamazepine (CBZ), while negligible for removal of benzoic acid (BA) and 4-nitrophenol (4-NP).

In a later study, Shih and co-workers proposed that it was the surface-bound sulfate radicals that attacked the contaminant in a Pd-Al_2O_3/PMS system [45]. The mineralized intermediates in phenol decomposition by the Pd-Al_2O_3/PMS were identified to be similar to that of the $SO_4^{\cdot -}$-dominated system (Co^{2+}/PMS) and the surface-confined sulfate radical was quantified by the probe reaction of methanol oxidation to formaldehyde. Besides, Yang et al. reported that carbon fibres (CFs) immobilized copper oxide (CuO-CFs) could simulate PMS to generate ROSs ($\cdot OH$, $SO_4^{\cdot -}$, and $^1O_2$) for catalytic oxidation [46]. The persistent free radicals (PFRs) in CFs played a crucial role in filling the Cu^{2+}/Cu^+ cycle and transferring electrons to O_2 toward $O_2^{\cdot -}$ for singlet oxygen evolution (Eq. (15)). Nie et al. also unveiled that singlet

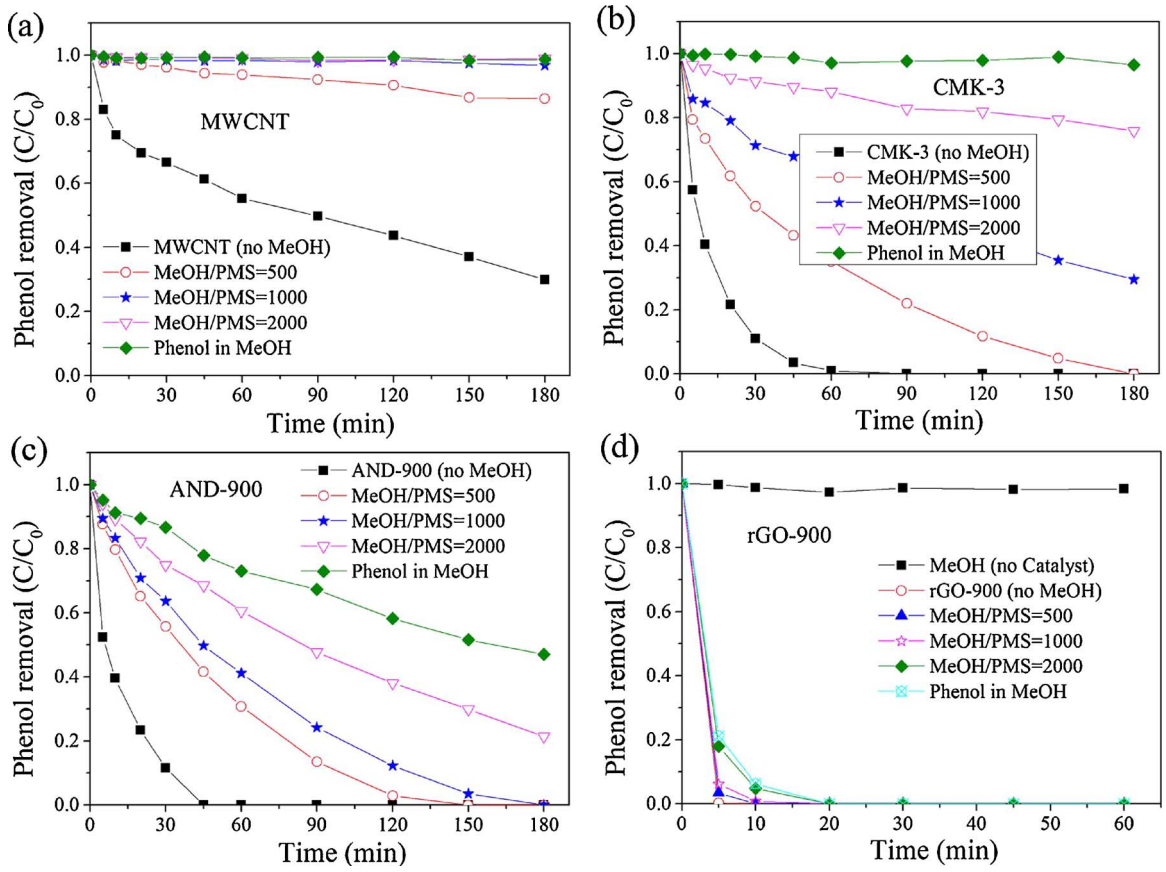

Fig. 2. Methanol (MeOH) quenching effect on phenol oxidation in different nanocarbon/PMS systems (a) multi-walled carbon nanotubes (MWCNTs), (b) cubic mesoporous carbon (CMK-3), (c) annealed nanodiamond (AND-900), and (d) reduced graphene oxide (rGO-900).

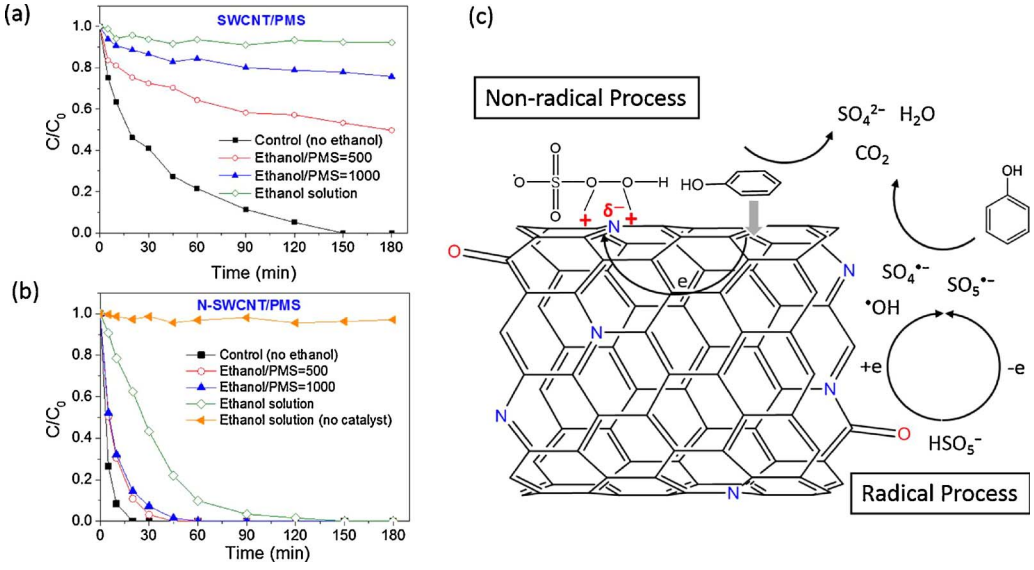

Fig. 3. Comparison of alcohol quenching effect in (a) SWCNT/PMS and (b) N-SWCNT/PMS systems, (c) illustration of N-doping induced nonradical oxidation on carbon nanotubes. Reprinted with permission from [22], Copyright 2015 American Chemical Society.

oxygen was the primary ROS from PMS activation on magnetic Cu^0/Fe_3O_4 composites [47]. In that study, the zero valence copper functioned as an *electron shuttle* from organic to PMS, which synergistically promoted the production of singlet oxygen from PMS for contaminant degradation.

2.2. Nonradical reaction in PDS activation

Zhang et al. first discovered that CuO/PDS is highly effective for decomposition of 2,4-dichlorophenol (2,4-DCP). In the reactions, addition of ethanol and chloride could barely impact the oxidation efficiencies, suggesting a novel oxidative mechanism not dominated by the sulfate radicals [23]. The authors proposed that PDS molecules tend to react with the positively charged CuO surface via intimate outer-sphere interaction without PDS dissociation, and that the activated PDS molecules directly attack 2,4-DCP via electron abstraction. Trace level radicals (·OH, $SO_4^{\cdot -}$) were also detected by *in situ* EPR in the CuO/PDS system by Du et al., however, the nonradical process was still

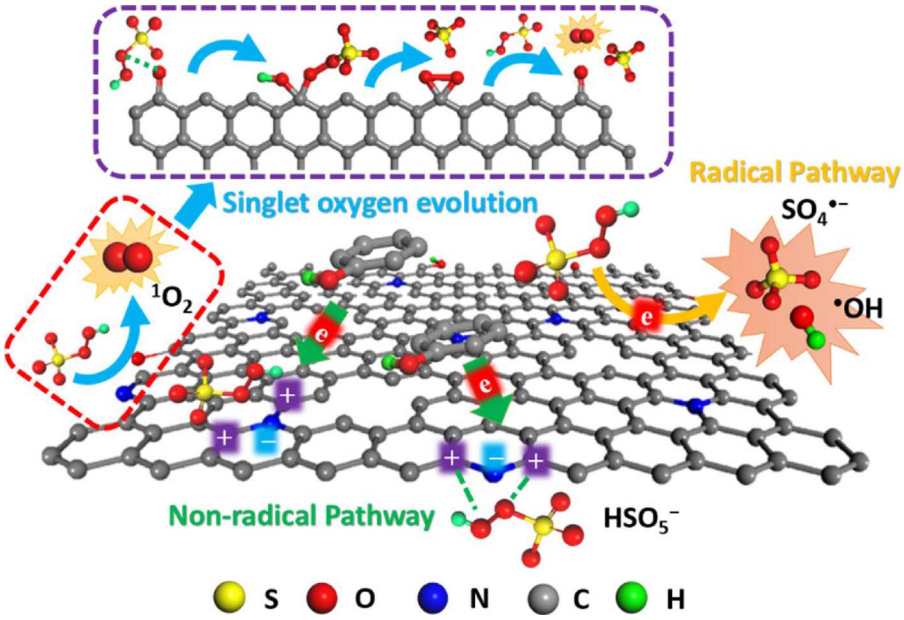

Fig. 4. Illustration of different reaction pathways of PMS activation for phenol degradation on N-doped graphene.

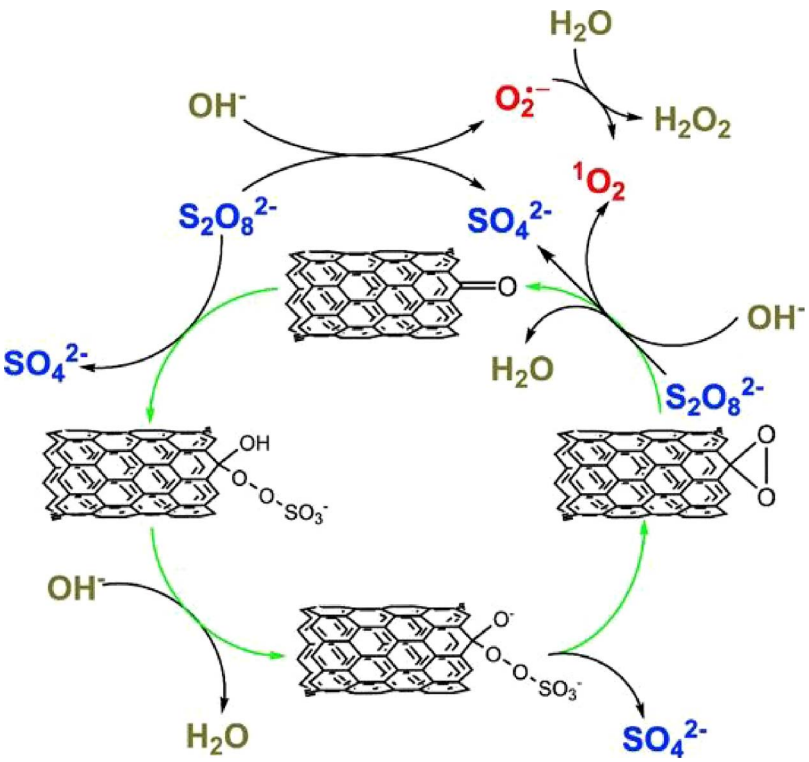

Fig. 5. Illustration of peroxydisulfate activation on carbon nanotubes to produce singlet oxygen.

verified to be the dominant pathway [48]. Additionally, Ma and co-workers reported that the carbamazepine could be oxidized on Ti/Pt anode in PDS solution by direct electrolysis and surface-activated PDS via a nonradical mechanism [49]. It was also reported that PDS molecules could be intercalated into a Mg/Al-layered double hydroxide (LDH) and activated by the basic sites for phenol oxidation, because the narrow space between LDH layers protected the activated PDS from cleaving into sulfate radicals and secured a nonradical pathway [50].

In a metal-free system, Tang and co-workers reported that N-doped reduced graphene oxide (N-RGO) could work as a bifunctional nanomaterial for adsorption and oxidation of phenolics [51]. The graphene surface-confined sulfate radicals were identified to be the dominant ROSs, which are inaccessible to the hydrophilic radical scavenger of methanol but could be quenched by a surface quenching agent of KI. Furthermore, the oxidative efficiency of N-RGO/PDS demonstrated a positively linear correlation with the adsorptive capacity of organics on graphene, implying that pre-adsorption of the phenolics was the key step for the organic to react with the surface-bounded sulfate radicals [51]. A similar nonradical mechanism was also found by Chen et al. [52] and Liu et al. [53] using N-doped/aminated graphene and N-doped porous carbon as PDS activators, respectively. Duan et al. unveiled that 0–3 dimensional nanocarbons (graphene, carbon nanotubes, annealed nanodiamond) could effectively activate PDS for catalytic oxidation with both free radicals and surface-attached sulfate radicals, and water oxidation was partially experienced as an important intermediate for PDS activation [54–56].

In addition, Lee et al. reported that PDS could be activated via outer-sphere interaction with the highly conjugated π system of carbon nanotubes (CNT) to form a reactive complex for selective oxidation of chlorophenols [57]. Cheng et al. reported that PDS activation on Fe/S modified CNT followed a similar mechanism [58]. Moreover, it was found that addition of iodide (I^-) could promote the decomposition of PDS-CNT complex to form hypoiodous acid (HOI) and sulfate anions (SO_4^{2-}) [59]. Similarly, the addition of chlorine (Cl^-) in CNT/PMS was able to transfer the oxidation from a sulfate radical-dominated system to a nonradical process for dye removal due to the formation of hypochlorous acid (HClO) [60]. The introduction of halogen ions inhibited the production of sulfate radicals via one-electron transfer and new oxidants (HOI and HClO) were generated by the organic oxidation. In a subsequent study, Cheng et al. integrated EPR spin trapping technique with chemical probes of 9,10-diphenylanthracene (DPA), furfuryl alcohol (FFA), and NaN_3, to conclude that the singlet oxygen was the primary reactive species for the organic degradation in PDS/CNT [61]. The carbonyl groups at the boundaries of CNT were supposed to be the active sites for generation of singlet oxygen as manifested in Fig. 5.

Kim and co-workers further reported that graphitized nanodiamonds (G-NDs) were able to be engaged as a charge-transfer-mediator that facilitates the electron transport from the organic to PDS via a graphitic sphere to achieve contaminant oxidation [62]. The G-NDs were reported to outperform other nanocarbons such as graphene and carbon nanotube. The graphitic degree of nanodiamonds partially determined the catalytic activity and some dubious sites, e.g. the doubling bonds, edging sites, and functional groups on the outer fullerene shell, also influence the activity [62–64]. Besides, free radicals (·OH, $SO_4^{\cdot -}$) have also been indicated to be responsible, at some extent, for the organic oxidation in G-NDs/PDS system, because the addition of radical quenching agents obviously decreased the reaction rate constant [56,63].

2.3. Nonradical reaction in other oxidative systems

Apart from persulfate-based AOPs, nonradical reaction was also reported in other AOPs. Choi and co-workers observed the production of singlet oxygen from periodate (IO_4^-) in alkaline solutions via Eqs. (18)–(19), and the system was effective for selective degradation of cimetidine (CMT) and ranitidine (RANI) [65]. The FFA oxidation kinetics reveal that 1 mol of FFA degradation requires 3 mol of periodate, which was supported by the proposed mechanism that 1 mol singlet oxygen was generated accordingly. Moreover, the addition of aromatic substances with vicinal hydroxyl groups (i.e. catechol) in periodate/base was beneficial for singlet oxygen evolution due to the formation of unstable catalytic intermediate with adjacent oxygen radical pairs (neighboring Ph-O·), whereas the hydroxyl groups in meta-position (resorcinol) and para-position (hydroquinone) were ineffective because of the stable quinone intermediates. Yao's group investigated the hemin-functionalized MWCNTs for catalytic decomposition of pollutants with H_2O_2 [66]. It was unveiled that the hemin served as an electron sink to transport the unpaired electrons from the persistent free radicals of MWCNTs for H_2O_2 reduction, meanwhile leaving the oxidative holes on the carbon surface for dye bleaching as shown in Fig. 6.

$$3IO_4^- + 2OH^- \rightarrow 3IO_3^- + 2O^{\circ}_2^- + H_2O \quad (18)$$

$$IO_4^- + 2O^{\circ}_2^- + H_2O \rightarrow IO_3^- + 2^1O_2 + 2OH^- \quad (19)$$

Nonradical oxidation phenomenon was also observed in ozone-based AOPs, which have been widely believed as hydroxyl radical-based systems. Zhang et al. reported that cerium supported palladium oxide (PdO/CeO) could dissociate O_3 molecules into surface adsorbed reactive species for oxalate mineralization without producing hydroxyl radicals [67]. The CeO_2 support was witnessed to be able to impact the binding affinity of Pd ions to the dissociated intermediates such as atomic oxygen (*O) and peroxide ($*O_2$), which rapidly attacked the adjacent oxalate-CeO_2 complex. Ma et al. also suggested that catalytic ozonation of nitrobenzene mainly occured on the surface of granular activated carbon immobilized manganese oxides (MnO_x/GAC), whereas hydroxyl radicals were not the primary oxidative species [68]. Furthermore, Wang et al. reported that $O_2^{\cdot -}$ and singlet oxygen were the ROS in graphene-catalyzed ozonation and account for *p*-hydroxylbenzoic acid (PHBA) degradation [69].

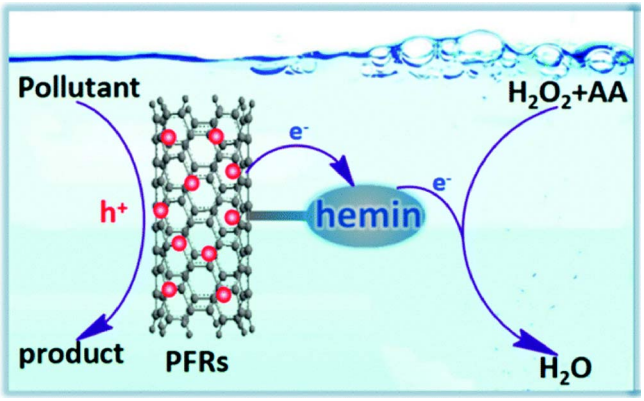

Fig. 6. The hole-oxidation mechanism in hemin-MWCNT/ascorbic acid (AA)/H_2O_2 system. Reproduced from [66] with permission from the Royal Society of Chemistry.

3. Mechanism of nonradical oxidation

3.1. Intrinsic active species in the nonradical oxidation

As illustrated above, nonradical reaction occurs in different systems involved in varying catalysts and oxidants. A summary of the catalytic systems and reactive species identified in the nonradical systems is listed in Table 1. It can be seen that versatile mechanisms were proposed for the nonradical-based AOPs, including singlet oxygen [40,61], surface activated complex [22,23], surface-confined sulfate radicals [51,56] or atomic oxygen [67], as well as a surface electron-transfer mechanism (catalyst as an electron conductor) [55,62]. Different reaction pathways were even proposed for the similar catalytic systems in different studies. For instance, PDS/CNT has been identified as a nonradical system, whereas the activated PDS complex [57] or singlet oxygen [61] was identified to be the dominant oxidative species in this system from the two studies. Moreover, Zhang et al. reported that PDS could be activated on CuO surface to form a reactive complex that directly attacked the target organics [23]. However, in Pd@Al_2O_3/PMS [44] and graphitized nanodiamond (G-ND)/PDS [62] systems, the catalysts were believed to serve as an electron bridge (or conductor) to facilitate the charge transport from the co-adsorbed organic (the electron donor) to oxidants (PMS or PDS, the electron acceptor) through the surface region of the catalyst. A surface-bonded-$SO_4^{\cdot -}$ mechanism was also proposed for the nonradical processes in N-doped graphene/PDS [51,52] and G-ND/PDS [56]. Therefore, it is still controversial if the surface reactive intermediates (activated oxidants or surface-bound species) directly attack the organic, or the catalyst serves as the electron-tunnel to promote the electron transport from the adsorbed contaminants to the surface-activated oxidant via continuously electron-transfer processes within the conductor. However, it is also possible that different mechanisms could be involved and mirrored by the adsorptive behaviors of the organics and oxidants on the catalysts. For instance, PMS decomposition on Pt@Al_2O_3 required the co-existence of the organics implying the electron-tunnelling mechanism, whereas the bare carbocatalysts (CNT, G-ND) could achieve PMS/PDS decomposition to some extent in the absence of the contaminants, suggesting a different nonradical pathway (surface activated complex) [44,57,62]. Though great efforts have been made to unveil the mystery of nonradical routes, the intrinsic interaction between the oxidants and

Table 1
A summary of the mechanism and characteristics of nonradical-based catalytic systems.

Entry	Oxidant	Catalysts	Reactive species /Oxidative pathway	Degradable organic (high reaction rate)	Undegradable Organic (moderate/low reaction rate)	References
1	PMS	Benzoquinone	$^1O_2$	sulfamethoxazole	benzoic acid (low), atrazine (low)	[24]
2	PMS	NaOH	$O_2^{\cdot -}$, $^1O_2$	acid orange 7	–	[28]
3	PMS	Polyphosphates (pH = 9.5)	$O_2^{\cdot -}$, $^1O_2$	acid orange 7	–	[29]
4	PMS	Graphene, Annealed nanodiamond	·OH, $SO_4^{\cdot -}$, surface activated PMS (dominant for graphene)	phenol, catechol, methylene blue, sulfachlorophyridazine	–	[32,79]
5	PMS	N-SWCNT	·OH, $SO_4^{\cdot -}$, surface activated PMS complex (dominant)	phenol	–	[22]
6	PMS	N-graphene	·OH, $SO_4^{\cdot -}$, $^1O_2$ (dominant)	p-hydroxylbenzoic acid, phenol, sulfachlorophyridazine, 2,4,6-trichlorophenol	–	[40,41]
7	PMS	N-graphene	·OH, $SO_4^{\cdot -}$, $^1O_2$, surface activated PMS complex	p-hydroxylbenzoic acid, phenol	benzoic acid (moderate), nitrobenzene (moderate),	[42]
8	PMS	N−CNT	·OH, $SO_4^{\cdot -}$, $^1O_2$, surface activated PMS complex (dominant)	phenol	–	[43]
9	PMS	Pd/Al_2O_3, Pd/TiO_2	Surface electron-transfer mechanism	phenol, 4-chlorophenol, 2,4,6-trichlorophenol	bisphenol A (moderate), carbamazepine (moderate), benzoic acid (low), 4-nitrophenol (low)	[44]
10	PMS	Pd/Al_2O_3	Surface-bound $SO_4^{\cdot -}$	1,4-dioxane	–	[45]
11	PMS	CuO−CFs	·OH, $SO_4^{\cdot -}$, $^1O_2$ (dominant)	acid red 1, acid orange 7, methylene blue, rhodamine B,8-hydroxyquinonline	phenol (moderate), sulfamethoxazole (moderate), benzoic acid (low)	[46]
12	PMS	Cu^0/Fe_3O_4	$^1O_2$, Surface electron-transfer mechanism	rhodamine B, methylene blue, orange II, phenol, 4-chlorophenol	–	[47]
13	PMS	Ti/Pt anode	Surface activated PMS complex	carbamazepine, sulfamethoxazole, propranolol, benzoic acid	atrazine, nitrobenzene	[49]
14	PDS	N-graphene	Surface-bound $SO_4^{\cdot -}$	Bisphenol A, Bisphenol F	2,4-dichlorophenol (moderate), 4-chlorophenol (moderate), phenol (low)	[51]
15	PDS	N-graphene, NH_2-graphene	Surface-bound $SO_4^{\cdot -}$	sulfamethoxazole	–	[52]
16	PDS	Annealed nanodiamond	·OH, $SO_4^{\cdot -}$, Surface-bound $SO_4^{\cdot -}$	phenol	nitrobenzene(low), benzoic acid(low)	[56]
17	PDS	Graphitized nanodiamond	Surface electron-transfer mechanism	phenol, aniline, Bisphenol A, acetaminophen, sulfamethoxazole, ranitidine, carbamazepine	benzoic acid(low)	[62]
18	PDS	MWCNT, SWCNT	Surface activated PDS complex	phenol, BPA, acetaminophen, carbamazepine, propranolol, sulfamethoxazole, 4-chlorophenol, 2,4,6-trichlorophenol	nitrobenzene(low), benzoic acid(low), furfuryl acid (low)	[57]
19	PDS	Fe/S-CNT	Surface activated PDS complex	2,4-dichlorophenol	–	[58]
20	PDS	MWCNT	$^1O_2$	2,4-dichlorophenol	–	[61]
21	PDS	Cubic mesoporous carbon	Surface electron-transfer mechanism	phenol	–	[80]
22	PDS	CuO	Surface activated PDS complex	phenol, 2,4-dichlorophenol, 2,4,6-trichlorophenol trichloroethylene,	p-chlorobezoic acid (low), iopromide (low)	[23]
23	PDS	CuO	·OH, $SO_4^{\cdot -}$, Surface activated PDS complex (dominant)	p-chloroaniline	–	[48]
24	KIO_4	KOH, NOMs/KOH	$^1O_2$	cimetidine, ranitidine,	propranolol (moderate), Bisphenol A (low), 4-chlorophenol (low)	[65]
25	H_2O_2	hemin-MWCNT/AA	Hole oxidation	reactive red M3-BE	–	[66]
26	O_3	PdO/CeO_2	Surface atomic oxygen	oxalate	–	[67]
27	O_3	MnO_x/GAC	Surface activated O_3 complex	nitrobenzene	–	[68]
28	O_3	graphene	$O_2^{\cdot -}$, $^1O_2$	p-chlorobezoic acid	–	[69]

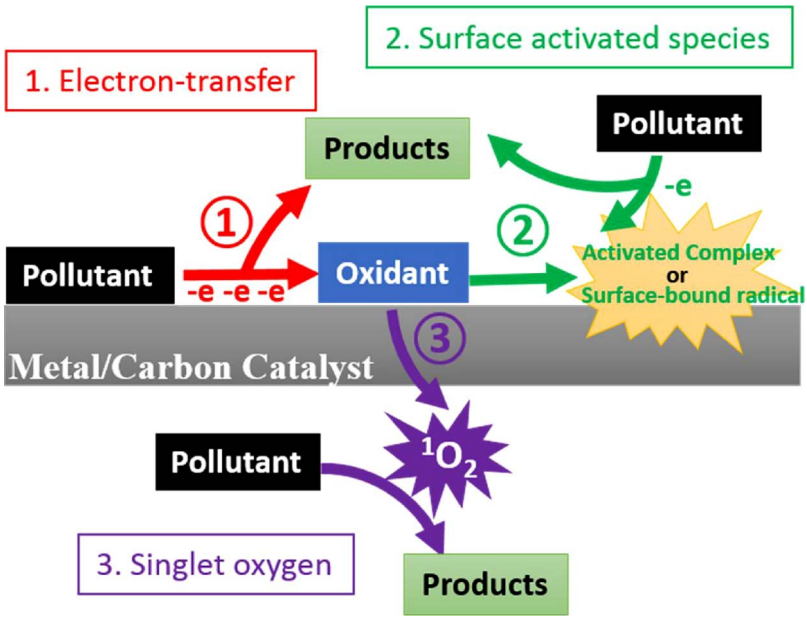

Fig. 7. Illustration of nonradical mechanisms for catalytic oxidation of organic contaminants in AOPs. (The oxidant would be PMS, PDS, H_2O_2, or O_3).

catalysts during the activation has not been probed with direct and solid evidences. As summarized in Table 1, Fig. 7 presents an illustration of three dominant reaction pathways in nonradical processes with surface activated complex (or surface-confined radical), electron-transfer process, and involvement of singlet oxygen for catalytic oxidation of organic contaminants.

In light of the complicated factors in experiments and materials, *in situ* characterization techniques (Raman, FTIR, and EPR etc.) may be helpful for on-line monitoring the transition states of the activated superoxides, the interactions with the organic, as well as the organic mineralization pathways to elucidate the intrinsic reactive species. However, it can be sure that the nonradical processes usually exhibit a mild oxidative potential compared with the free radicals, and oxidize the organic via electron-transfer, either through the catalyst conductor or directly with the reactive intermediates. Herein, the nonradical pathway as a surface confined reaction is more selective to oxidize the electron-rich substances compared with the free radicals. Such a nonradical process also favors a stronger affinity of the organics with the catalyst. Therefore, the nature of organic substrates was found to significantly impact the adsorptive capacity, and influence the nonradical oxidation efficiency [51].

3.2. The nature of catalysts determining the reaction pathway

The surface of the catalysts might intrinsically affect their interactions with the superoxides toward a radical or nonradical process. For heterogeneous metals/oxides-based catalysis, the catalytic activity is significantly dependent on the valence states, size, morphology, crystalline structure, and grain boundaries, which subsequently determine the redox potential and binding strength of the metal sites to react with PMS/PDS. For instance, Ahn et al. reported that a low loading level (1.0 wt.%) of Pd nanoparticles on Al_2O_3 would act as an electron-bridge for charge-transfer between co-adsorbed PMS and organic pollutants on Pd surface [44]. In such a process, PMS was barely consumed without the presence of the organic. However, when Pd loading was increased to 10 wt.% with a larger particle size, the reactive species in Pd/Al_2O_3/PMS were confirmed to be the surface-confined $SO_4^{\cdot -}$ that directly oxidized the contaminants [45]. Therefore, the particle size can partially determine the organic oxidation pathway with Pd/PMS. Besides, CuO obtained via a one-pot pyrolysis (450 °C) of copper salts would activate PDS via a complete nonradical mechanism [23], while CuO synthesized by a two-stage treatment at lower temperatures (150 and 300 °C) could produce a small amount of hydroxyl and sulfate radicals [48]. The metal oxides from different synthesis procedures exhibited varying catalytic behaviors, despite that the crystal structures of CuO in the two studies are not systematically compared. Moreover, the molecular difference of PMS with an asymmetric structure (HO—O—SO_3) compared with the symmetric PDS (SO_3—O—O—SO_3) gives rise to the unbalanced charge densities of the oxygen atoms in the peroxide O—O bond. Herein, PMS is more sensitive to the polarized carbon regions introduced by N-doping with greater adsorption affinity in carbon-based nonradical processes. Theoretically, in the nonradical processes, strong binding and moderate charge transfer are experienced between the catalyst and oxidants so that the peroxides are activated/confined on the surface without instantly releasing the free radicals to the bulk solution. Therefore, the coordination chemistry and electronic culture of the catalysts can dominate the binding behavior and tendency for electron donation between the surface atoms and oxidants, then consequently affecting the reactivity of the activated intermediates to react with organics. Higher activity of a catalyst toward redox reaction will easily induce radical generation from an oxidant while nonradical process will generally occur on the catalyst with less redox potential by forming a surface complex.

Moreover, nonradical systems exhibit different selectivity toward the pollutants (Table 1**)** because the oxidation effectiveness was simultaneously decided by the oxidative capacity of the reactive species and organic substrates. Apart from the adsorption capacity of an organic on a catalyst, the reactivity of the organic molecules also depends on electronic properties of the molecular structure for the electrophilic reaction in the nonradical pathways. For instance, the adsorption capacity, ionization potential (IP), and redox potential of the organic substrates after the first-step oxidation synergistically determined the selectivity and overall mineralization in the nonradical processes [51,70]. Then, it would be not perplexing that chemicals such as nitrobenzene and benzoic acid with the benzene ring functioned with deactivating groups (or electron withdrawn groups, such as $-NO_2$ or $-COOH$) were not favorable for a nonradical reaction, whereas the electron-rich substances such as dyes, phenol/chlorophenols, and big molecule antibiotics could be rapidly oxidized via electron abstraction by the nonradical reactive species.

The mechanism of AOPs with carbocatalysis is more complicated since the commercial carbon materials (e.g. carbon nanotubes) used in the aforementioned studies are not from the same source, leading to the intrinsical differences in the structure and surface chemistry. For

instance, compared with the metal-driven PDS decomposition, the scenarios become more dramatic for CNT/PDS systems because three different mechanisms of radical [71], nonradical (surface activated PDS complex) [57], and singlet oxygen [61] have been proposed with experimental supports in each case. Generally, commercial nanocarbons are simultaneously functionalized with diverse oxygen moieties, defective sites, and reductive degree, not to mention the fact that the electronic features of carbon atoms in different dimensions and matrix were synergistically manipulated by the distinct graphitic degree, curvature structure, hybrid effect (multi-layers), and carbon configurations (sp, sp^2, or sp^3 hybridization). These features substantially govern the electron states and spin culture of the carbocatalysts with versatile active centers that might induce different mechanisms or simultaneously initiate multiple reaction pathways at different sites on the same catalyst. Thus huge differences would be observed with different materials in the same system. Therefore, the integration of deliberate material-design, *in situ* characterizations, and theoretical calculation to monotonously investigate a simplified model/structure would be much helpful to exclusively illustrate a specific active site and simulate reaction pathways toward a radical/nonradical reaction. Additionally, the effect of metal residual induced during the synthesis of carbon materials cannot be ruled out in the carbon-catalyzed AOPs. The trace level of metal/oxides would be incorporated into the graphitic carbon framework or encapsulated under the carbon layer, which can hardly be eliminated by a facile pre-treatment of thorough acid washing and can be detected in an atomic scale by the sensitive elemental analysis such as X-ray photoelectron spectroscopy (XPS) as reported in the studies [72].

3.3. Critical methods to confirm the generation of singlet oxygen

Singlet oxygen, as a high-energy form of oxygen, is a reactive oxidant produced from photosensitization, which has been widely used for photodegradation, organic synthesis, and photodynamic therapy [73,74]. Interestingly, singlet oxygen was also found in AOPs, which manifested a mild and selective oxidation capacity toward pollutants and resistance to the popular free radical scavengers such as methanol and tert-butanol. Hence, the characteristics of singlet oxygen in AOPs are quite similar to the nonradical reactive intermediates such as activated persulfates or surface-confined radicals in light of selectivity and oxidative potential. It was found that singlet oxygen could be universally generated from PMS (activated by base [28], benzoquinone [24], and graphene [42]), PDS (activated by carbon nanotubes [61]), and periodate (activated by base [65]) by non-photochemical approaches. In these studies, singlet oxygen was identified by using sodium azide (NaN_3) as the quenching agent and spin trapping by 2,2,6,6-tetramethyl-4-piperidone (TMP) on electron paramagnetic resonance (EPR), which displays characteristic triplet peaks. Unfortunately, both the techniques have some limitations to exclusively identify the singlet oxygen. Firstly, it has been unveiled that superoxide radical ($O_2^{\cdot -}$) can react with TMP to produce similar triplet peaks as singlet oxygen [75,76]. Thus, EPR trapping technique cannot distinguish these two reactive species with TMP, to exclusively confirm the presence of singlet oxygen without the co-existence of superoxide radical. Superoxide radical is also insensitive to the popular radical quenching agents, such as methanol, ethanol, or tert-butanol. The impact of superoxide radical cannot be simply excluded by alcohol quenching, because most singlet-oxygen based studies witnessed superoxide radical involved. Moreover, the addition of p-BQ or nitroblue tetrazolium as the superoxide radical scavengers can dramatically slow down or even terminate the oxidation in these studies, making it more difficult to distinguish if the superoxide radical only serves as the intermediate for singlet oxygen generation (Eq. (16)) or the dominant reactive species [28,29,46,65,69].

It should be also pointed out that TMP, the trapping agent of singlet oxygen, is an alkaline chemical in nature, thus the dosage of the trapping agent and pH environment should be carefully controlled in EPR tests, otherwise base activation may take place to generate $^1O_2$ and/or $O_2^{\cdot -}$ to mislead the results. Additionally, sodium azide as a strong reducing agent can react with not only singlet oxygen but also hydroxyl and sulfate radicals, and the reaction of NaN_3 with superoxide radical or surface activated complex is still unclear. Therefore, the recognition of singlet oxygen from a simple method of TMP trapping or chemical quenching need to be carefully interpreted as the results may not exclude the impacts of other reactive species.

Chemical probes of furfuryl alcohol (FFA) [28,29,46] and diphenylanthracene (DPA) [24,61] have be used for identifying singlet oxygen, nevertheless, the reactions of the two probe compounds toward the nonradical complex and free radicals (especially for superoxide radical) are still yet to be investigated. Other techniques such as fluorescent probes and photosensitizers can also be helpful to confirm the existence of singlet oxygen [77,78]. In conclusion, it would be suggested that multi-strategies be integrated for tracing the occurrence and determination of the particular role of singlet oxygen in the nonradical oxidation.

4. Prospective and implications

Currently, nonradical reaction has been believed to occur with radical reaction in several catalytic AOPs for water treatment. In the nonradical-based processes, the reactive species (such as the activated oxidant-catalyst complex, surface-bound sulfate radicals, or singlet oxygen) were supposed to be highly reactive electrophiles and exhibit a milder oxidative potential compared with free radicals, ·OH and $SO_4^{\cdot -}$. Therefore, the nonradical systems are more selective to the electron-rich substances and the catalytic activity is dependent on the texture and adsorptive capacity of the organic substrates as well as the properties of the catalysts. Such an oxidative capacity is able to readily oxidize the contaminants at the initial stage. However, complete decomposition of the organics in water may still require a combined radical/nonradical system, because the free radicals are more capable of mineralizing the oxidized by-products into carbon dioxide and water to achieve a desirable removal efficiency of total organic carbon.

Nevertheless, the nonradical system can be utilized for pre-treatment of highly hazardous industrial, pharmaceutical and agricultural disposers, which can be devastating to the bacteria in the bioprocessing treatment. Previous studies indicated that the nonradical-dominated systems have several advantages in adaption to diverse pH circumstances (acidic/neutral/basic), resistance to the versatile inorganic ions, halogens, as well as background organic matters due to the selectivity and moderate redox potential [23,24,42]. These substances universally exist in domestic sewage and industrial wastewaters, which are believed to be detrimental to the free radicals in Fenton and Fenton-like systems. It is also reported that carbonyl groups [24] and vicinal hydroxyl functionalities [65] in natural organic matters (NOMs) could promote the generation of singlet oxygen for enhancing oxidation efficiency, which is highly favorable for the application of the nonradical oxidation for *in situ* chemical oxidation (ISCO) in remediation of rivers, lakes, and underground water. Besides, the novel oxidative system is promising for the selective removal of trace target organics in complicated water matrix or high-salinity water.

It should be pointed out that recent nonradical processes are mostly discovered in the persulfate-based systems, whereas the investigations with other peroxides such as hydrogen peroxide, ozone, and periodate are still limited. This may provide more research opportunities in novel nonradical systems for future studies. Many studies unveiled that multiple reaction pathways may exist in the catalytic systems which simultaneously involve radical and nonradical reactions. However, it is still challenging to precisely and quantitatively estimate the contribution of the nonradical pathway in total oxidation. It is also of great significance to investigate if the proportion of nonradical pathway can be rationally controlled by tuning the properties of the catalysts or

simply regulating the reaction conditions [79]. Since the mechanisms of nonradical processes remain ambiguous and controversial, systematic studies are still encouraged to design more efficient catalysts, to investigate the intrinsic catalytic sites, and improve the stabilities. More importantly, comprehensive understanding is required from more studies on the distinctions between radical and nonradical/singlet oxygen based oxidation in terms of selectivity, oxidative potential, degradation pathways and toxicity of the novel system, to pursue future environmental implications.

Acknowledgement

The authors acknowledge financial support from the ARC Discovery Projects (DP150103026).

References

[1] Z. Du, S. Deng, S. Zhang, W. Wang, B. Wang, J. Huang, Y. Wang, G. Yu, B. Xing, Environ. Sci. Technol. 51 (2017) 8027–8035.
[2] M. Rebhun, S. Meir, Y. Laor, Environ. Sci. Technol. 32 (1998) 981–986.
[3] T.A. Ternes, M. Meisenheimer, D. McDowell, F. Sacher, H.J. Brauch, B.H. Gulde, G. Preuss, U. Wilme, N.Z. Seibert, Environ. Sci. Technol. 36 (2002) 3855–3863.
[4] D. Brown, P. Laboureur, Chemosphere 12 (1983) 405–414.
[5] G. Vidal, A. Carvalho, R. Mendez, J.M. Lema, Bioresour. Technol. 74 (2000) 231–239.
[6] D.C. Stuckey, P.L. Mccarty, Water Res. 18 (1984) 1343–1353.
[7] R. Andreozzi, V. Caprio, A. Insola, R. Marotta, Catal. Today 53 (1999) 51–59.
[8] M. Pera-Titus, V. Garcia-Molina, M.A. Banos, J. Gimenez, S. Esplugas, Appl. Catal. B 47 (2004) 219–256.
[9] S. Esplugas, J. Gimenez, S. Contreras, E. Pascual, M. Rodriguez, Water Res. 36 (2002) 1034–1042.
[10] M.A. Oturan, J. Peiroten, P. Chartrin, A.J. Acher, Environ. Sci. Technol. 34 (2000) 3474–3479.
[11] M. Klavarioti, D. Mantzavinos, D. Kassinos, Environ. Int. 35 (2009) 402–417.
[12] P.D. Hu, M.C. Long, Appl. Catal. B 181 (2016) 103–117.
[13] P. Neta, R.E. Huie, A.B. Ross, J. Phys. Chem. Ref. Data 17 (1988) 1027–1284.
[14] F. Gozzo, J. Mol. Catal. A 171 (2001) 1–22.
[15] I. Yamazaki, L.H. Piette, J. Am. Chem. Soc. 113 (1991) 7588–7593.
[16] S. Rahhal, H.W. Richter, J. Am. Chem. Soc. 110 (1988) 3126–3133.
[17] J.D. Rush, W.H. Koppenol, J. Am. Chem. Soc. 110 (1988) 4957–4963.
[18] D.H.R. Barton, D. Doller, Acc. Chem. Res. 25 (1992) 504–512.
[19] L. Deguillaume, M. Leriche, N. Chaurnerliac, Chemosphere 60 (2005) 718–724.
[20] F. Shi, M.K. Tse, Z.P. Li, M. Beller, J. Chem. Eur. 14 (2008) 8793–8797.
[21] S.J. Hug, O. Leupin, Environ. Sci. Technol. 37 (2003) 2734–2742.
[22] X.G. Duan, H.Q. Sun, Y.X. Wang, J. Kang, S.B. Wang, ACS Catal. 5 (2015) 553–559.
[23] T. Zhang, Y. Chen, Y. Wang, J. Le Roux, Y. Yang, J.-P. Croué, Environ. Sci. Technol. 48 (2014) 5868–5875.
[24] Y. Zhou, J. Jiang, Y. Gao, J. Ma, S.Y. Pang, J. Li, X.T. Lu, L.P. Yuan, Environ. Sci. Technol. 49 (2015) 12941–12950.
[25] A.R. Gallopo, J.O. Edwards, J. Org. Chem. 46 (1981) 1684–1688.
[26] J.O. Edwards, R.H. Pater, R. Curci, F. Di Furia, Photochem. Photobiol. 30 (1979) 63–70.
[27] A. Lange, H.-D. Brauer, J. Chem. Soc. Perkin Transact. 2 (1996) 805–811.
[28] C.D. Qi, X.T. Liu, J. Ma, C.Y. Lin, X.W. Li, H.J. Zhang, Chemosphere 151 (2016) 280–288.
[29] X.Y. Lou, C.L. Fang, Z.N. Geng, Y.M. Jin, D.X. Xiao, Z.H. Wang, J.S. Liu, Y.G. Guo, Chemosphere 173 (2017) 529–534.
[30] H.Q. Sun, S.Z. Liu, G.L. Zhou, H.M. Ang, M.O. Tade, S.B. Wang, ACS Appl. Mater. Interfaces 4 (2012) 5466–5471.
[31] X.G. Duan, H.Q. Sun, Z.M. Ao, L. Zhou, G.X. Wang, S.B. Wang, Carbon 107 (2016) 371–378.
[32] X.G. Duan, Z.M. Ao, L. Zhou, H.Q. Sun, G.X. Wang, S.B. Wang, Appl. Catal. B 188 (2016) 98–105.
[33] S. Indrawirawan, H.Q. Sun, X.G. Duan, S.B. Wang, Appl. Catal. B 179 (2015) 352–362.
[34] K. Nakada, M. Fujita, G. Dresselhaus, M.S. Dresselhaus, Phys. Rev. B 54 (1996) 17954–17961.
[35] D.E. Jiang, B.G. Sumpter, S. Dai, J. Chem. Phys. 127 (2007) 124703.
[36] H.Q. Sun, Y.X. Wang, S.Z. Liu, L. Ge, L. Wang, Z.H. Zhu, S.B. Wang, Chem. Commun. 49 (2013) 9914–9916.
[37] S. Indrawirawan, H.Q. Sun, X.G. Duan, S.B. Wang, J. Mater. Chem. A 3 (2015) 3432–3440.
[38] X.G. Duan, Z.M. Ao, H.Q. Sun, S. Indrawirawan, Y.X. Wang, J. Kang, F.L. Liang, Z.H. Zhu, S.B. Wang, ACS Appl. Mater. Interfaces 7 (2015) 4169–4178.
[39] X.G. Duan, K. O'Donnell, H.Q. Sun, Y.X. Wang, S.B. Wang, Small 11 (2015) 3036–3044.
[40] P. Liang, C. Zhang, X. Duan, H. Sun, S. Liu, M.O. Tade, S. Wang, Environ. Sci. Nano 4 (2017) 315–324.
[41] P. Liang, C. Zhang, X.G. Duan, H.Q. Sun, S.M. Liu, M.O. Tade, S.B. Wang, ACS Sustain. Chem. Eng. 5 (2017) 2693–2701.
[42] D. Li, X. Duan, H. Sun, J. Kang, H. Zhang, M.O. Tade, S. Wang, Carbon 115 (2017) 649–658.
[43] C. Wang, J. Kang, P. Liang, H.Y. Zhang, H.Q. Sun, M.O. Tade, S.B. Wang, Environ. Sci. Nano 4 (2017) 170–179.
[44] Y.Y. Ahn, E.T. Yun, J.W. Seo, C. Lee, S.H. Kim, J.H. Kim, J. Lee, Environ. Sci. Technol. 50 (2016) 10187–10197.
[45] Y. Feng, P.-H. Lee, D. Wu, K. Shih, Water Res. 120 (2017) 12–21.
[46] Z. Yang, D. Dai, Y. Yao, L. Chen, Q. Liu, L. Luo, J. Chem. Eng. 322 (2017) 546–555.
[47] G. Nie, J. Huang, Y. Hu, Y. Ding, X. Han, H. Tang, Chinese J. Catal. 38 (2017) 227–239.
[48] X. Du, Y. Zhang, I. Hussain, S. Huang, W. Huang, J. Chem. Eng. 313 (2017) 1023–1032.
[49] H. Song, L. Yan, J. Ma, J. Jiang, G. Cai, W. Zhang, Z. Zhang, J. Zhang, T. Yang, Water Res. 116 (2017) 182–193.
[50] X. Huang, M. Su, J. Zhou, W. Shu, Z. Huang, N. Gao, G. Qian, Chem. Eng. J. (2017).
[51] X.B. Wang, Y.L. Qin, L.H. Zhu, H.Q. Tang, Environ. Sci. Technol. 49 (2015) 6855–6864.
[52] H. Chen, K.C. Carroll, Environ. Pollut. 215 (2016) 96–102.
[53] N. Liu, L. Zhang, Y. Xue, J. Lv, Q. Yu, X. Yuan, Sep. Purif. Technol. 184 (2017) 213–219.
[54] X.G. Duan, H.Q. Sun, J. Kang, Y.X. Wang, S. Indrawirawan, S.B. Wang, ACS Catal. 5 (2015) 4629–4636.
[55] X.G. Duan, Z.M. Ao, H.Q. Sun, L. Zhou, G.X. Wang, S.B. Wang, Chem. Commun. 51 (2015) 15249–15252.
[56] X.G. Duan, C. Su, L. Zhou, H.Q. Sun, A. Suvorova, T. Odedairo, Z.H. Zhu, Z.P. Shao, S.B. Wang, Appl. Catal. B 194 (2016) 7–15.
[57] H. Lee, H.J. Lee, J. Jeong, J. Lee, N.B. Park, C. Lee, J. Chem. Eng. 266 (2015) 28–33.
[58] X. Cheng, H.G. Guo, Y.L. Zhang, Y. Liu, H.W. Liu, Y. Yang, J. Colloid Interf. Sci. 469 (2016) 277–286.
[59] C.T. Guan, J. Jiang, C.W. Luo, S.Y. Pang, C.C. Jiang, J. Ma, Y.X. Jin, J. Li, Environ. Sci. Technol. 51 (2017) 479–487.
[60] J.B. Chen, L.M. Zhang, T.Y. Huang, W.W. Li, Y. Wang, Z.M. Wang, J. Hazard. Mater. 320 (2016) 571–580.
[61] X. Cheng, H. Guo, Y. Zhang, X. Wu, Y. Liu, Water Res. 113 (2017) 80–88.
[62] H. Lee, H.I. Kim, S. Weon, W. Choi, Y.S. Hwang, J. Seo, C. Lee, J.H. Kim, Environ. Sci. Technol. 50 (2016) 10134–10142.
[63] X. Duan, H. Sun, S. Wang, Environ. Sci. Technol. 51 (2017) 5351–5352.
[64] J.A. Zhang, D.S. Su, R. Blume, R. Schlogl, R. Wang, X.G. Yang, A. Gajovic, Angew. Chem. Int. Ed. 49 (2010) 8640–8644.
[65] A.D. Bokare, W. Choi, Environ. Sci. Technol. 49 (2015) 14392–14400.
[66] B. Jiang, D.J. Dai, Y.Y. Yao, T.F. Xu, R.H. Li, R.J. Xie, L.K. Chen, W.X. Chen, Chem. Commun. 52 (2016) 9566–9569.
[67] T. Zhang, W.W. Li, J.P. Croue, Environ. Sci. Technol. 45 (2011) 9339–9346.
[68] J. Ma, M.H. Sui, T. Zhang, C.Y. Guan, Water Res. 39 (2005) 779–786.
[69] Y.X. Wang, Y.B. Xie, H.Q. Sun, J.D. Xiao, H.B. Cao, S.B. Wang, ACS Appl. Mater. Interfaces 8 (2016) 9710–9720.
[70] P. Hu, H. Su, Z. Chen, C. Yu, Q. Li, B. Zhou, P.J.J. Alvarez, M. Long, Environ. Sci. Technol. 51 (2017) 11288–11296.
[71] H.Q. Sun, C. Kwan, A. Suvorova, H.M. Ang, M.O. Tade, S.B. Wang, Appl. Catal. B 154 (2014) 134–141.
[72] D.S. Su, G.D. Wen, S.C. Wu, F. Peng, R. Schlogl, Angew. Chem. Int. Ed. 56 (2017) 936–964.
[73] M.C. DeRosa, R.J. Crutchley, Coordin. Chem. Rev. 233 (2002) 351–371.
[74] C. Schweitzer, R. Schmidt, Chem. Rev. 103 (2003) 1685–1757.
[75] R. Poupko, I.J. Rosentha, Phys. Chem. 77 (1973) 1722–1724.
[76] T.A. Konovalova, J. Lawrence, L.D. Kispert, J. Photochem. Photobiol. A 162 (2004) 1–8.
[77] R. Ruiz-González, A.L. Zanocco, Singlet Oxygen (2016) 103–120.
[78] Y.Y. Yuan, C.J. Zhang, S.D. Xu, B. Liu, Chem. Sci. 7 (2016) 1862–1866.
[79] X. Duan, Z. Ao, H. Zhang, M. Saunders, H. Sun, Z. Shao, S. Wang, Appl. Catal. B 222 (2018) 176–181.
[80] X. Duan, H. Sun, M. Tade, S. Wang, Catal. Today (2017), http://dx.doi.org/10.1016/j.cattod.2017.04.038.